Energy &
Environmental Science

RSC Publishing

PAPER

View Article Online
View Journal



Cite this: DOI: 10.1039/c3ee00019b

# Fungal cellulases and complexed cellulosomal enzymes exhibit synergistic mechanisms in cellulose deconstruction†

Michael G. Resch,*[ab] Bryon S. Donohoe,[ab] John O. Baker,[ab] Stephen R. Decker,[ab] Edward A. Bayer,[c] Gregg T. Beckham[de] and Michael E. Himmel[ab]

Received 4th January 2013
Accepted 8th April 2013

DOI: 10.1039/c3ee00019b

www.rsc.org/ees

Nature has evolved multiple enzymatic strategies for the degradation of plant cell wall polysaccharides, which are central to carbon flux in the biosphere and an integral part of renewable biofuels production. Many biomass-degrading organisms secrete synergistic cocktails of individual enzymes with one or several catalytic domains per enzyme, whereas a few bacteria synthesize large multi-enzyme complexes, termed cellulosomes, which contain multiple catalytic units per complex. Both enzyme systems employ similar catalytic chemistries; however, the physical mechanisms by which these enzyme systems degrade polysaccharides are still unclear. Here we examine a prominent example of each type, namely a free-enzyme cocktail expressed by the fungus *Hypocrea jecorina* and a cellulosome preparation secreted from the anaerobic bacterium *Clostridium thermocellum*. We observe striking differences in cellulose saccharification exhibited by these systems at the same protein loading. Free enzymes are more active on pretreated biomass and in contrast cellulosomes are much more active on purified cellulose. When combined, these systems display dramatic synergistic enzyme activity on cellulose. To gain further insights, we imaged free enzyme- and cellulosome-digested cellulose and biomass by transmission electron microscopy, which revealed evidence for different mechanisms of cellulose deconstruction by free enzymes and cellulosomes. Specifically, the free enzymes employ an ablative, fibril-sharpening mechanism, whereas cellulosomes physically separate individual cellulose microfibrils from larger particles resulting in enhanced access to cellulose surfaces. Interestingly, when the two enzyme systems are combined, we observe changes to the substrate that suggests mechanisms of synergistic deconstruction. Insight into the different mechanisms underlying these two polysaccharide deconstruction paradigms will eventually enable new strategies for enzyme engineering to overcome biomass recalcitrance.

## Broader context

Industrial conversion of plant biomass into transportation fuels will likely be a vital component of the global renewable energy portfolio to reduce both greenhouse gas emissions and fossil fuel utilization for mankind's energy needs. However, plants have evolved considerable defense mechanisms against deconstruction of their cell wall polysaccharides into sugars, and as such, depolymerization to sugars for subsequent biological or catalytic conversion to fuels remains a significant technical challenge with major cost implications in biomass conversion. In nature, many microorganisms evolved a strategy wherein plant cell wall-active enzymes are secreted as a cocktail of individual enzymes that work synergistically to depolymerize biomass, referred to as a "free enzyme" paradigm. Some ruminal microorganisms conversely evolved a strategy wherein their plant cell wall-active enzymes are tethered to large scaffolds, which are linked to the cells for sugar production in close proximity for uptake, termed the "cellulosome". Here, we mechanistically compare the free enzyme and cellulosome paradigms, and we show that these enzyme systems use dramatically different mechanisms to degrade biomass at the nanometer scale. Overall, this study highlights new opportunities for mixing these two systems for enhanced industrial performance and suggests that there may be an optimal strategy between these two mechanisms.

[a]*Biosciences Center, National Renewable Energy Laboratory, 15013 Denver West Parkway, Golden, CO, 80401, USA. E-mail: michael.resch@nrel.gov; Fax: +1 303-384-6363; Tel: +1 303-903-8934*

[b]*BioEnergy Science Center (BESC), National Renewable Energy Laboratory, 15013 Denver West Parkway, Golden, Colorado, 80401, USA*

[c]*Department of Biological Chemistry, The Weizmann Institute of Science, Rehovot, 76100, Israel*

[d]*National Bioenergy Center, National Renewable Energy Laboratory, 15013 Denver West Parkway, Golden, Colorado, 80401, USA*

[e]*Department of Chemical Engineering, Colorado School of Mines, Golden, Colorado, 80401, USA*

† Electronic supplementary information (ESI) available: Detailed methods, results from additional digestions and TEM imaging, results from various control experiments. See DOI: 10.1039/c3ee00019b

## Introduction

Plant cell walls represent a vast, renewable carbon source in the biosphere, and as a result, several enzymatic strategies have evolved to deconstruct structural plant polysaccharides.[1–8] These enzymatic strategies rely largely on glycoside hydrolases, oxidative enzymes,[7,9] and other enzymes. Many organisms secrete "free enzyme" cocktails wherein various proteins diffuse independently of one another and, *via* different substrate specificities,[10] work synergistically to degrade biomass. These free enzymes range from systems in which the enzymes contain one catalytic unit up to systems in which there are several catalytic units per protein molecule. In particular, the well-characterized fungus *Hypocrea jecorina* (*Trichoderma reesei*) secretes a potent cocktail of free carbohydrate-active enzymes to degrade cellulose and hemicellulose.[5,8] *H. jecorina* and closely related organisms typically secrete enzymes with only one catalytic unit per protein. As with most bacteria and fungi that utilize a free enzyme paradigm, the majority of protein mass-produced by *H. jecorina* consists of processive cellulases. Distinct families of processive cellulases have evolved to hydrolyse cellulose from either the reducing or non-reducing end.[11,12] Processive (exo-acting) cellulases are complemented by endoglucanases and oxidative enzymes[7,9] that cleave cellulose at points in the interior of the chains to expose free ends for attachment and detachment of processive enzymes. Co-secreted hemicellulases target the variety of glycosidic linkages in hemicellulose and work in conjunction with esterases, pectinases, and various other enzymes. Generally, once exposed to pretreated biomass, free enzymes exploit openings in the cell wall matrix to degrade their target cell wall components.

In contrast to free enzyme systems, an alternative degradation paradigm has evolved in certain bacteria and fungi in which multiple biomass-degrading enzymes are physically linked *via* a protein scaffold. This self assembling macromolecular enzyme complex, termed the cellulosome, was first discovered in the anaerobic bacterium, *Clostridium thermocellum*.[13] In contrast to the *H. jecorina* cellulase cocktail, the cellulosome paradigm represents a contrast to (known) biomass degradation strategies wherein many catalytic units are linked to form a mega-Dalton (MDa) complex. Cellulosomes incorporate processive and non-processive cellulases, hemicellulases, and other carbohydrate-active enzymes onto large proteins known as scaffoldins. The specific, noncovalent attachment of cellulosomal enzyme dockerins to cohesins of the scaffoldin enables enzyme co-localization. The primary scaffoldin, CipA, can bind up to nine enzymes *via* Type I cohesins, which are complementary to the Type I dockerins linked to individual enzymes.[14,15] Primary scaffoldins also typically contain a carbohydrate binding module (CBM) and a Type II dockerin domain.[14] Up to seven primary scaffoldins, along with their associated enzymes, can attach through Type II dockerins to Type II cohesins of secondary scaffoldins to form complexes incorporating as many as 50 to 60 catalytic units per cellulosome.[16] These secondary scaffoldins can in turn adhere to bacterial cells or exist freely in solution.[17] Cellulosomes can facilitate diverse assemblies of enzymes and CBMs with aggregate molecular masses up to 10 MDa. The proximity of CBMs and carbohydrate-active enzymes with multiple binding preferences and substrate specificities, respectively, bound to long, flexible scaffoldins has been hypothesized to impart "plasticity" (variable quaternary structure) to the cellulosome, a characteristic which in turn has been hypothesized to yield enhanced activity.[6]

The organization of catalytic units and CBMs in the cellulosome is significantly different from the free enzymes and, as described here, this structural difference translates into strikingly different enzymatic performance on different substrates. Specifically, free fungal enzymes are significantly more active on thermochemically treated biomass than are cellulosomes, whereas the cellulosomes have a dramatic advantage in the digestion of pure cellulose. Transmission electron microscopy (TEM) imaging of partially digested cellulose reveals that cellulosomes employ a mechanism that is different from the well-known fibril sharpening, ablative mechanism of free cellulases.[18,19] Instead of fibril sharpening, cellulosomes appear to splay open one end of cellulose bundles, increasing the separation distance between cellulose microfibrils. Deeper understanding of these two distinct mechanisms of biomass degradation will eventually enable new approaches to engineering enzymes and cocktails for digestion of the variety of substrates relevant to the developing biofuels industry.

## Results

### Development of optimal reaction conditions for cellulosome activity

To compare the activity of the free and complexed enzyme systems in an unbiased manner, we isolated high molecular weight (HMW) cellulosomes from the *C. thermocellum* culture filtrate, and then optimized their activity. For isolation, we used affinity purification[20] and size exclusion chromatography (SEC) to separate the HMW cellulosomes (>1 MDa) from the non-cellulosomal and aggregated proteins (Fig. S1†). SEC purification of HMW cellulosome from the original broth increased the Avicel conversion significantly compared to that of the entire secretome (Fig. S2†). We used this purified fraction in all of the experiments described hereafter. To optimize the reaction conditions, we examined three variables known to influence cellulosomal activity and stability: oxygen sensitivity,[21] stabilization by calcium,[22–24] and cellobiose inhibition.[25,26] Optimal cellulosomal activity was achieved when digestions contained L-cysteine as a reducing agent, $CaCl_2$ for stabilization, and β-D-glucosidase to mitigate cellobiose inhibition (Fig. S3†).

### Cellulosomes degrade cellulose faster than free cellulases

To examine the different mechanisms of the free and complexed enzyme systems on model cellulose substrates, we compared cellulosome performance to that of a commercial *H. jecorina* enzyme preparation, Cellic CTec2 (Novozymes). Fig. S4† shows an SDS-PAGE of CTec2 and the *C. thermocellum* cellulosomal system for comparison of the compositions of these protein

 

cocktails. We measured the performance of both enzyme systems on two model cellulose substrates: Avicel PH-101 and Whatman #1 filter paper. These two substrates are primarily crystalline cellulose with varying degrees of polymerization (DP). For both systems, we used an enzyme loading of 5 mg of protein per gram of cellulose in 1% (w/v) substrate slurry. From Fig. 1A and B, cellulosomes are considerably more efficient at converting crystalline cellulose with either low (Avicel PH-101, Fig. 1A) or high DP (Whatman #1 filter paper, Fig. 1B) than are free enzymes. Using Avicel that is 74% crystalline,[27] the cellulosomes reach 100% conversion in 100 h, compared to ~50% conversion by the free enzymes. Cellulosomes are also significantly more effective on Whatman #1 filter paper than CTec2 (Fig. 1B). These data demonstrate that cellulosomes are superior at degrading crystalline cellulose, whether with high or low DP.

### Free enzymes are more effective than cellulosomes at hydrolyzing pretreated biomass

We also compared the cellulosomes and free enzymes in the hydrolysis of untreated (Fig. S5†) and dilute-acid-pretreated (Fig. 1C and D) biomass substrates. We found that cellulosomes and free enzymes exhibit a similar ability to degrade knife milled, 0.5 mm sieved, non-pretreated switchgrass (Fig. S5†). The low conversion reflects the limited accessibility of the cellulose and hemicellulose in non-pretreated biomass to enzymes.

We then compared activities of cellulosomes and free enzymes on switchgrass and poplar thermally pretreated with dilute sulphuric acid, as shown in Fig. 1C and D, respectively. Dilute sulphuric acid pretreatment results in the hydrolysis and solubilisation of hemicelluloses, and removal of some lignin from the cell wall, a fraction of which condenses on cell wall surfaces upon cooling the reactor. These combined effects result in cell wall delamination.[28] The switchgrass and poplar samples were knife milled, pretreated with dilute sulphuric acid, and extensively washed to remove soluble sugars, degradation products, and other soluble components. In stark contrast to the comparatively poor performance of free enzymes on crystalline cellulose where cellulosomes are more effective, free enzymes are dramatically faster at hydrolyzing pretreated biomass at the same enzyme mass loading (Fig. 1C and D). The inactivity of the cellulosome is apparent after the first 24 h of the reaction. To determine if cellulosomes were limited by the lack of cellulose accessibility, we varied the enzyme loading

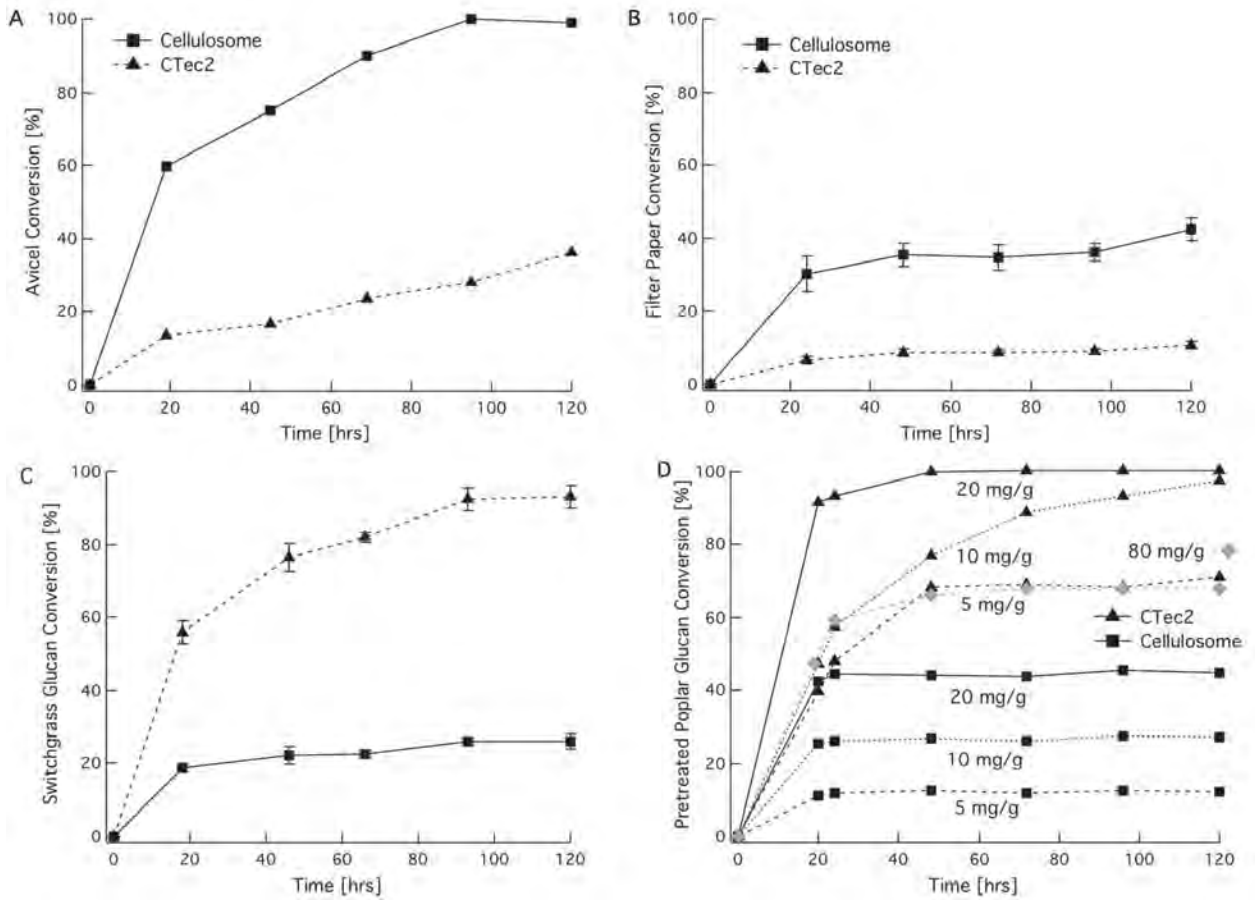


**Fig. 1** Comparison of cellulosomes and free enzymes in the digestion of cellulose and biomass substrates. Enzymatic digestion of (A) Avicel and (B) Whatman filter paper by HMW cellulosomes and Cellic CTec2 (Novozymes). Digestions shown in A and B were loaded with 5 mg per g of cellulose in 1% (w/v) cellulose slurries. In enzymatic digestions of (C) dilute-acid pretreated switchgrass and (D) dilute-acid pretreated poplar with cellulosomes and Cellic CTec2 (Novozymes), cellulases were loaded at 20 mg per g of cellulose in the switchgrass digestion (C), and in (D), cellulosomes and CTec2 were compared at protein loadings of 5, 10, and 20 mg per g of cellulose. The gray curve represents digestion of pretreated poplar loaded with 80 mg per g cellulosomes. Digestions of pretreated biomass were conducted with 2% (w/v) solids slurries.

from 5 to 20 mg per g cellulose and measured the conversion over 120 h (Fig. 1D). We found that the cellulose conversion increases with an increase in enzyme loading, which suggests that the reactive sites on the biomass surfaces are not fully saturated at the loadings tested in this study. We also determined that the supplementation of the cellulosome preparation with purified hemicellulases did not increase glucan release from pretreated switchgrass (Fig. S6†).

Additionally, we varied the cellulosome loading to determine if there was a threshold loading that yielded the same conversion as that of the lowest loading of free enzymes. For pretreated poplar, a cellulosome loading of 80 mg per g of glucan achieves the same conversion level as that of CTec2 at 5 mg per g (diamonds, Fig. 1D). Using these data, one can compare on a molar basis the free enzymes and cellulosome complexes required to achieve the same hydrolytic effect. Assuming a molecular weight average of 60 kDa for the free enzyme mixture and 1000 kDa per cellulosome complex, these loadings of 80 mg cellulosome per g cellulose and 5 mg "free enzymes" per g cellulose are roughly equivalent to 0.8 micromoles of protein (or complex) per g of cellulose in each case.

### Cellulosomes increase the surface area accessible to enzymatic attack by separating cellulose microfibrils

To investigate the morphological changes caused by the digestion of crystalline cellulose by free enzymes or cellulosomes, we isolated Avicel from digestions with approximately 65% of the cellulose removed. Digested Avicel particles were applied directly to a carbon coated TEM grid, negatively stained, and imaged. Both samples displayed particles ranging in size from 3 to 580 $\mu m^2$ in cross-sectional area with many of the particles still too thick to allow electron transmission without further sample preparation. Our analysis focused on the smallest (0.5 μm to 2 μm wide), most electron-translucent particles, in which individual cellulose microfibrils could be delineated within the bundles. Among this class of particles, there was a consistent pattern in the geometry of the particle ends. As previously observed,[18,19] the particles digested with the free enzymes displayed one end that was tapered to a narrow point (Fig. 2A–D). The angle of the taper ranged from −6 to −12° measured between the particle edge and the long axis of the particle. The free enzymes appear to ablate the surface of cellulose microfibril bundles and work preferentially on one end only. The end of the particle opposite the tapered end was always either a blunt edge nearly perpendicular to the long axis of the particle or at an angle of ∼60° (Fig. 2A′–D′).

In contrast, the Avicel particles digested with cellulosomes did not display a tapered end, but instead exhibited highly irregular and splayed end morphology (Fig. 2E–H). The angle of the splayed microfibrils ranged from 5 to 22° measured as a deflection away from the long axis of the particle. In the cellulosome samples the end opposite the splayed end was either blunt, or at an angle up to ∼45° from the long axis of the particle (Fig. 2E′–H′). By measuring the perimeter of the particles in these two dimensional TEM micrographs as an approximation of the accessible surface area within 1 μm of the tapered or splayed end of the digested particles, we calculate an almost 2-fold higher surface area (Fig. S7†) in the splayed ends compared to tapered ends. This suggests that cellulosomes employ a mechanism distinct from the ablative mechanism of free cellulases, in that they separate individual cellulose microfibrils from crystalline cellulose particles for localized attack.

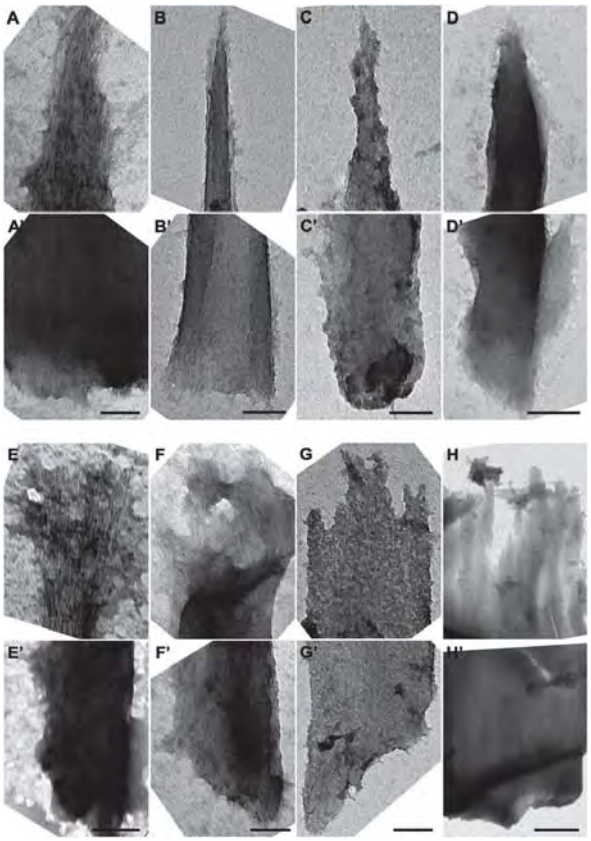


**Fig. 2** TEM micrographs of Avicel particles digested with free enzymes or cellulosomes. Each paired image set is of the opposite ends of the same particle. Avicel was digested to a cellulose conversion of ∼65% with free enzymes for 120 h (A–D) and with cellulosomes for 24 h (E–H). Particles in the free enzyme samples display narrow, tapered ends (A–D) and blunt or angled ends (A′–D′). In contrast, Avicel particles digested with cellulosomes display irregular, splayed ends (E–H) and blunt or angled ends (E′–H′). Scale bars A–C, F, G = 200 nm, D, H = 500 nm, E = 100 nm.

### Free and cellulosomal systems exhibit different enzyme localization on pretreated biomass

In addition to the imaging on enzyme-digested Avicel, we also investigated morphological changes in pretreated switchgrass digested by free enzymes or cellulosomes. We preserved these samples by high-pressure freezing and freeze-substitution to keep structural details as close as possible to the structures present during digestion and to retain the antigenicity of enzyme epitopes for immuno-localization studies. The pretreated samples imaged before exposure to cellulosomes or free enzymes were already extensively fractured and delaminated due to milling and pretreatment (Fig. S8 and S9†). To visualize changes in the pretreated biomass during enzymatic digestion, we collected samples from the digestion reactions at 24 h. Despite the observed variability within the samples, it is clear

that the immuno-localization of enzyme penetration into the pretreated biomass provides significant insight. The distribution of Cel7A labelling in the free enzyme system shows that free enzymes have penetrated and dispersed into the secondary cell walls (Fig. 3A). Positive labelling for the cellulosome scaffoldin occurred only near fractures in the cell wall (Fig. 3B, arrow) or close to the cell wall surface (Fig. 3B′). These results suggest that accessibility to pretreated biomass is limited for the much larger, complexed enzymes.

### Free and complexed cellulases exhibit significant synergy in the digestion of crystalline cellulose

The results described above suggest that free cellulases and cellulosomes employ different physical mechanisms to break down recalcitrant polysaccharides. To determine if these two paradigms could be synergistic, we digested Avicel with a mixture of cellulosomes and free enzymes (Fig. 4). Cellulosomes and free enzymes were studied separately at loadings of 10 mg $g^{-1}$, as well as in mixtures of 5 mg $g^{-1}$ of each. The cellulosomes alone were assayed as noted above at their optimal conditions. The free cellulases alone were also assayed at their optimal conditions as described in the Methods section.[29] For the digestion of cellulose with the mixture of cellulases and cellulosomes, we carefully chose reaction conditions at which both systems maintain at least ~90% of their respective activity, as shown in Fig. S10† for the cellulosomes and described in ref. 29 for the free cellulase cocktail. We note that at 50 °C, the cellulosome activity is reduced by less than 10% compared to 60 °C (Fig. S10†). Interestingly, the combination of cellulosomes and free enzymes exhibited the highest activity on Avicel tested, reaching 100% conversion in 24 h. This performance can be compared to the cellulosomes, which reach 100% conversion in 48 h and the free enzymes, which are only able to digest 70% of the Avicel (Fig. 4A). These results suggest that these two mechanisms are complementary for the hydrolysis of crystalline cellulose. To investigate the mechanism of synergy between free and complexed enzymes, we conducted TEM imaging of Avicel that was 55% digested with the combination of enzyme systems (Fig. 4BI–IV). The cellulose particles digested using the combined enzymes displayed morphology dramatically different from those of particles digested with either of the systems alone. Free enzymes sharpen the cellulose ends, while cellulosomes cause splaying and surface area expansion. The combination of these two enzyme systems allowed

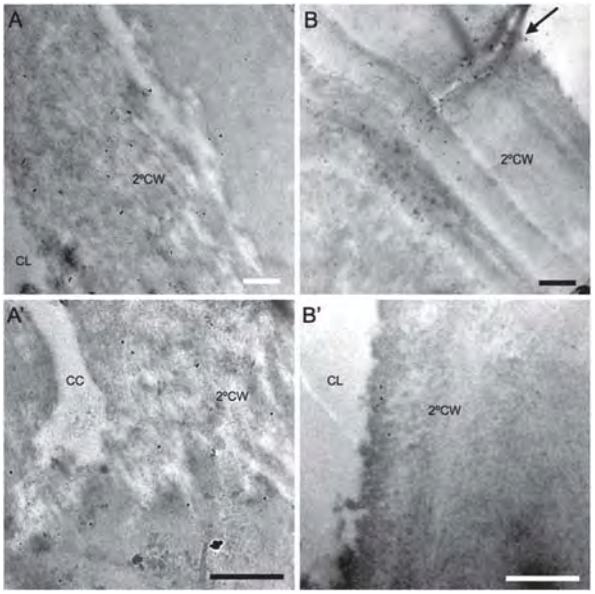


**Fig. 3** TEM micrographs of immuno-labeled dilute-acid pretreated switchgrass samples digested with free enzymes (A and A′) or cellulosomes (B and B′) for 24 h. The samples were immuno-labeled to localize Cel7A enzymes (A and A′) or the CBM3 on the cellulosome scaffold (B and B′), which appear as black spots (15 nm Au particles) in the micrographs. Cel7A was concentrated within several μm of the cell lumen (CL, A), after 24 h, the enzymes penetrate into the secondary cell walls (2° CW). The cellulosome scaffold CBM3 was found only near cell wall fractures (B, arrow) or very close to the cell wall surface (B′). Scale bars = 0.5 μm.

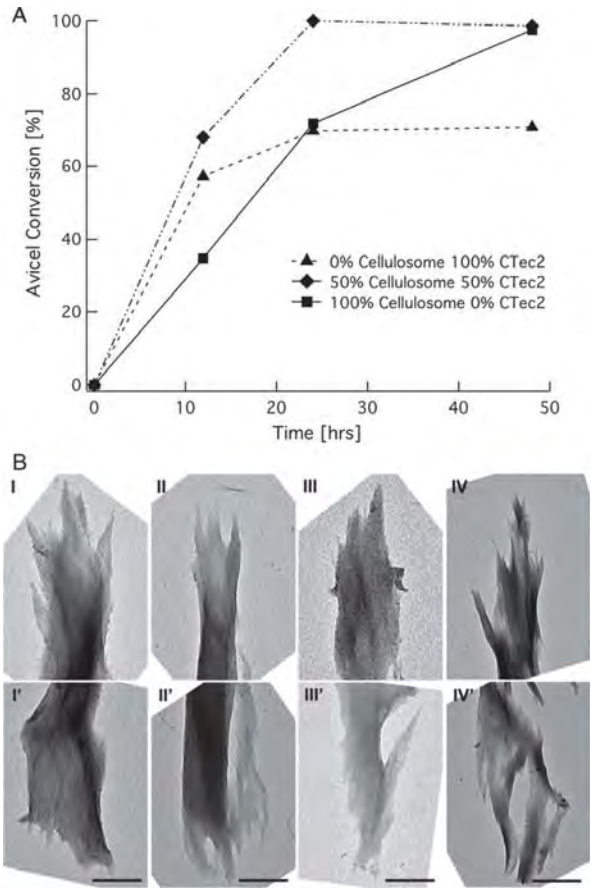


**Fig. 4** Synergistic effects of free enzymes and cellulosomes on Avicel examined by activity assays and TEM imaging. (A) Combinations of cellulosomes and free enzymes were loaded at 10 mg $g^{-1}$, and a mixture of 5 mg $g^{-1}$ of each was combined in enzymatic digestions of Avicel. The cellulosomes alone were assayed similarly to results presented in Fig. 1 and S3† at their optimal conditions, and the free cellulases alone were assayed at their optimal conditions as described in the Methods section.[29] For the combination of enzyme systems, we chose reaction conditions wherein the activity of both systems maintained at least 90% of their optimal activity, namely at 50 °C in 30 mM sodium acetate pH 5.5 buffer containing 10 mM $CaCl_2$, 100 mM NaCl, 2 mM EDTA, and 10 mM cysteine (Fig. S10†). Glucose and cellobiose release were measured every 12 h by HPLC. (B) Samples of the combined system were taken at a conversion level of ~55% for TEM image analysis. Image pairs are of opposite ends of the same particle. Scale bars = 500 nm.

deconstruction of the microfibril bundles deep into the particle (Fig. 4III′ and IV′). It is likely that the combination of surface ablation and fibrillation is the result of the two enzyme systems working in a complementary manner by exposing microfibril ends to enzyme action.

## Discussion

In this study, we compared the enzymatic digestion of cellulose and biomass substrates by a free enzyme cocktail and by purified cellulosomes, as these two classes of enzyme cocktails represent leading enzyme cocktail candidates for the burgeoning biofuels industry. The free enzyme cocktail used here is primarily comprised of enzymes with a single catalytic unit and CBM. In contrast, the cellulosomes used here contain many catalytic units per individual complex, linked to a single CBM-bearing scaffoldin *via* cohesin–dockerin interactions. To gain further insights, we applied TEM imaging to Avicel and biomass samples at the same level of conversion by free or complexed enzymes. Somewhat surprisingly, among the smallest, most electron translucent digested particles, distinct particle end morphologies were discernable. The consistency of these dramatic shapes suggests that the microfibrils in this class of particle are largely parallel and not anti-parallel. This is consistent with particles derived from only a few lamina of the original fibre cell secondary cell wall. These images revealed a novel mechanism by which cellulosomes are able to increase the accessible surface area for degradation of Avicel by a factor of 2 over free enzymes by separating individual cellulose microfibrils from larger particles, which is illustrated in Fig. 5, and quantified in Fig. S7.† The free enzymes, in contrast, primarily act *via* an ablative mechanism.[18,19] These results suggest that, in general, free and complexed enzymes function *via* different mechanisms and over different critical length scales. In combination, these two mechanisms can act synergistically to deconstruct cellulose. By providing comparisons of free enzymes with one catalytic unit per protein and one of the largest known biomass-degrading enzyme complexes, these results generally define the range of physical mechanisms nature employs to deconstruct cellulose, which is of significant interest for engineering enhanced enzyme cocktails.

Individually, the free and complexed enzymes digest Avicel particles from a single end preferentially. It is well known that many fungal cellulase cocktails contain a reducing-end specific, Family 7 cellobiohydrolase for significant hydrolytic potential,[30] and it is therefore likely that the reducing end of the cellulose bundles is where free cellulases attack and sharpen the cellulose particles. Similarly, the cellulosomal system from *C. thermocellum* contains Family 48 cellobiohydrolases (*e.g.*, Cel48S).[17] Family 48 cellobiohydrolases also contribute significant hydrolytic potential as reducing-end specific cellobiohydrolases,[12] and are key enzymes in cellulosomal activity with reductions in activity of ~60% upon deletion of the Cel48S gene from *C. thermocellum*.[31] Thus it is likely that the cellulosomes also preferentially act from the reducing end.

A potential explanation for the different physical mechanisms of action *on clean cellulose* shown in Fig. 2 may be the result of significantly different off-rates for the free cellulases compared to the cellulosomes. Based on the high number of potentially engaged catalytic units and CBMs present in a single cellulosomal complex, it is likely that the cellulosome off-rate will be drastically lower than the off-rate of a much smaller, free cellulase for several reasons. First, a free cellulase (as defined in this study) can exhibit at most a CBM and a catalytic domain simultaneously engaged on cellulose, whereas a cellulosomal complex can potentially have several CBMs (both Type A and Type B)[32] and multiple catalytic units engaged concomitantly. Additionally, CBMs linked together have been shown to exhibit

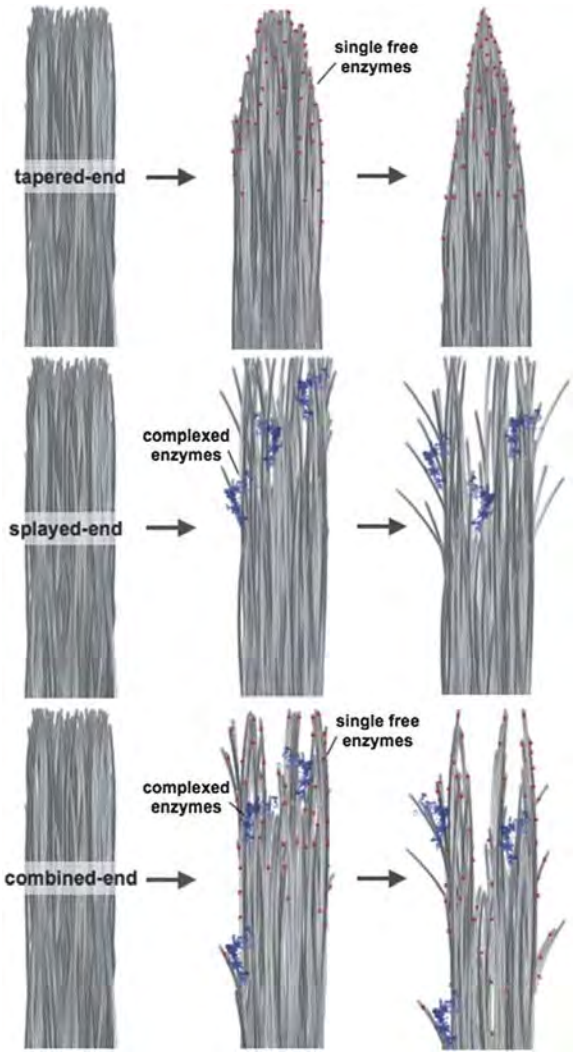


**Fig. 5** Illustration of the mechanisms by which free enzymes (top) and cellulosomes (middle) differ in their action on cellulose microfibril bundles and act synergistically to degrade cellulose (bottom). Free enzymes with one catalytic unit and a single CBM may be restricted to digesting only the surface of the crystalline cellulose microfibril bundles. The higher activity and processivity of the reducing-end-active enzymes in the complex lead to the overall tapered morphology. Conversely, complexed enzymes with multiple CBMs and catalytic domains likely exhibit lower off-rates and thus fully digest single microfibrils or regions of microfibrils leading to splaying of remaining undigested cellulose microfibrils. This in turn thereby increases the total substrate surface area available to enzymatic digestion. Accessibility to free microfibril ends that could be splayed would be limited in whole biomass by the presence of lignin and hemicellulose, which could explain why the performance of cellulosomes on intact biomass is compromised.

avidity effects, which can significantly enhance binding affinity by several orders of magnitude beyond the sum of individual CBMs alone.[32–35] Lastly, two recent studies on free cellulases have suggested the off-rate of catalytic domains is the rate-limiting step of cellulose hydrolysis by individual cellobiohydrolases, which would likely be amplified in the case of multiple catalytic domains linked together in a cellulosomal system, in a manner similar to observed CBM avidity.[36,37] Thus, cellulosomes contain multiple domains productively engaged on cellulose, which will most likely lead to significantly lower off-rates. Therefore cellulosomes are more likely to fully digest individual cellulose microfibrils or region of microfibrils before dissociation than free cellulases, which results in the splayed-end morphology observed in Fig. 2.

Furthermore, with respect to the mixture of free and cellulosomal enzymes shown in Fig. 4, it is likely that the mechanism of free cellulase/cellulosome synergy is one wherein the cellulosomes commit to a given microfibril or region of microfibrils, splay out the cellulose microfibrils by digesting away individual microfibrils from a bundle, and thereby expose more reactive surface area for free cellulase action. Thus, the free cellulase and cellulosome activities are synergistic, and not simply additive. An illustration of this hypothesis is shown in Fig. 5, which is a pictorial representation of the TEM images with cellulases labelled throughout the diagram.

With respect to the observations of free and complexed enzyme synergy, we note that the free enzyme cocktail used here contains lytic polysaccharide mono-oxygenases (LPMOs).[7,9,38–40] LPMOs require a reducing agent (either a small molecule reducing agent or cellobiose dehydrogenase), oxygen, and a Cu ion bound in the active site for activity. In the cellulose digestions wherein only free enzymes were used, no EDTA was added and the presence of cellobiose dehydrogenase in the enzyme cocktail and oxygen in the reaction buffer suggests that the LPMOs are active. In the synergy experiment between the free and complexed enzymes shown in Fig. 4, however, EDTA and cysteine were both added to the mixture, and thus a significant amount of LPMO activity is likely lost. However, we note that in Fig. 4A, even with the probable reduction or loss of LPMO activity, the free and complexed enzymes are still synergistic. Thus, the synergy between the free and complexed enzymes is likely primarily due to the relative mechanisms of the hydrolytic enzymes.

On pretreated biomass, multiple factors likely lead to the variations in observed enzyme localizations, which may also result in the different extents of biomass conversion. As it is likely that cellulosomes exhibit a substantially lower off-rate, it is probable that cellulosomes are active at their initial point of productive engagement on exposed surfaces of cellulose, as shown in Fig. 3. Moreover, Fig. 1D shows that the cellulosomal activity quickly plateaus, which may be the result of the low off-rate at the point of initial productive binding. In the case of cellulose with no other heterogeneities present, cellulosomes are able to fully digest the substrate. However, in the case of pretreated biomass, cellulosomes can likely become inactivated more easily because of reduced access to exposed cellulose. Free cellulases, on the other hand, with higher off-rates, can more readily diffuse to other regions of the biomass for productive engagement.

Another explanation that may contribute to the observed differences between free and complexed enzymes on pretreated biomass is the trapping of enzymes by binding to lignin. This trapping process would progressively remove enzymes able to digest cellulose from the population. Such an inactivation mechanism would almost certainly, as has been suggested by others,[41] affect the fungal enzymes as well as the cellulosomes. However, the much higher molecular weight of the cellulosome implies that for equal loadings on a mass basis, active cellulosomes would be present in much lower molar concentrations. Each nonproductive binding or trapping event may thus be expected to have a more dramatic negative effect on cellulosomal activity.

Lastly, we note that the free cellulase system used here is from an industrial enzyme cocktail expressed in *H. jecorina*, which contains enzymes with single CBMs and single catalytic domains. Although the enzyme activities of this cocktail are approximately known (Fig. S4†), the results in Fig. 2 are qualitatively equivalent to the ablative mechanism observed on microfibrils digested only with Family 7 cellobiohydrolases[18,19,42] which suggests that the GH7 cellobiohydrolase is the dominant activity present. As the objective of this study was to compare free and complexed cellulase systems, and as the mechanism employed by the free cellulase cocktail is as previously observed, the detailed composition of the free cocktail is not directly germane to the results obtained here.

In conclusion, this study implies that two of the most thoroughly studied and distinct paradigms of biomass degradation, namely free enzymes with single catalytic units per protein molecule, and multi-enzyme cellulosomes, function *via* different biophysical mechanisms to deconstruct recalcitrant cell wall polysaccharides, despite employing similar component enzymes and CBMs. The results from TEM imaging, activity measurements, and synergy studies suggest that cellulosomes work by separating individual microfibrils from large cellulose particles, which allows for localized enzymatic attack. Conversely, the free enzymes examined here and used in commercial enzyme cocktails display a longer critical length scale for ablative action down single microfibrils, and hence sharpen or taper both the cellulose particles and individual cellulose microfibrils simultaneously. Since the two paradigms represent the extremes of the known continuum of enzymatic biomass degradation, this study suggests that smaller enzyme complexes with multiple catalytic units and multiple CBMs per protein (but smaller than the cellulosome) may employ strategies with characteristics of both mechanisms. These findings highlight new potential opportunities for exploiting these two paradigms and suggest that an optimum synergy between these two mechanisms may be obtained by employing enzyme systems with selected characteristics of both natural paradigms.

## Methods

### Isolation of the HMW cellulosomes

*C. thermocellum* was grown on Avicel PH-101 and the cellulosome-containing sample was isolated according to ref. 43 (ESI text). The composition of the cellulosome is known from two

detailed mass spectrometry studies to vary only slightly (measured by enzymatic activity on cellulose) when grown on pretreated biomass or Avicel.[17,44] Purified cellulosomes were run on an SDS-PAGE shown in Fig. S4.† The primary protein present in the cellulosome is the 200 kDa CipA scaffoldin protein with several more components at lower molecular weight.

### Fungal cellulases

CTec2 preparation number NS-22086 PPC 30604 was obtained from Novozymes. The concentrated enzyme mixture was applied to an AKTA FPLC (GE) using a HiPrep 26/10 Sephadex (GE) desalting column to remove stabilizers and other additives that interfere with BCA protein assay and HPLC sugar quantification. Protein concentration was measured by BCA (Pierce). An SDS-PAGE for CTec2 is shown in Fig. S4.† Along with many standard fungal cellulase and hemicellulase activities, CTec2 contains oxidative enzymes,[45] which rely on the presence of cellobiose dehydrogenase[39,46] or the presence of reducing agents for activity.[7,9] To ensure that the activity of the free, oxidative enzymes did not rely on the presence of externally added reducing agent, a control experiment was conducted wherein ascorbic acid was added. Fig. S11† shows that the addition of ascorbic acid does not impact the free cellulase cocktail activity on clean cellulose.

### Cellulose substrates

Whatman #1 filter paper and Avicel PH-101 (Sigma-Aldrich) were suspended in nanopure $H_2O$ under vacuum overnight at 4 °C and washed three times with nanopure water by centrifugation at 500 × *g* to remove soluble sugars. Pellets were re-suspended to 20 mg $mL^{-1}$ (w/w) in 30 mM sodium acetate buffer, pH 5.0, containing 0.001% (w/v) sodium azide.

### Biomass preparation

Poplar and switchgrass biomass were pretreated in a continuous reactor according to ref. 47. The switchgrass was pretreated at 190 °C with a sulphuric acid loading of 50 mg per g dry solids, at an estimated residence time of 1 min. The solids loading in the pretreatment reactor was 25% (w/w). Poplar pretreatment conditions were 195 °C, 30 mg acid per g dry biomass, 1 min residence time and 25% (w/w) total solids. Pretreated solids were washed three times with nanopure water by centrifugation at 500 × *g*. Pellets were re-suspended to 20 mg $mL^{-1}$ (w/w) in 30 mM sodium acetate buffer, pH 5.0, containing 0.001% (w/v) sodium azide.

### Activity assays

The enzyme activity of the cellulosomes alone was assayed at 60 °C in 30 mM sodium acetate pH 5.5 buffer containing 10 mM $CaCl_2$, 100 mM NaCl, 2 mM EDTA, and 10 mM cysteine. Fungal cellulase (CTec2) activity alone was measured at 50 °C in 20 mM sodium acetate, pH 5.0. Mixtures of cellulosomes and CTec2 were assayed at 50 °C in 20 mM sodium acetate pH 5.5 buffer containing 10 mM $CaCl_2$, 100 mM NaCl, 2 mM EDTA and 10 mM cysteine. In all cases, pH was measured after combining the reaction components. Digestions were conducted in sealed 2 mL HPLC vials with continuous mixing by inversion at 10–12 $min^{-1}$. Unless otherwise noted, substrates were loaded at 10 mg dry biomass per mL in 1.4 mL reaction volumes. Representative (with respect to both solid and liquid phases of the digestion slurry) 0.1 mL samples were withdrawn from well-mixed digestion mixtures at selected time-points during the digestions and diluted 10-fold with deionized water into 2.0 mL HPLC vials that were then crimp-sealed and immersed in a boiling-water bath for 10 min to inactivate the enzymes and terminate the reaction. The diluted and terminated digestion aliquots were then filtered through 0.2 μm nominal-pore-size nylon syringe-filters (Pall/Gelman Acrodisc-13) to remove residual substrate and, presumably, most of the denatured enzyme. Released cellobiose and glucose in the diluted samples were then determined by HPLC analysis on an Aminex HPX-87H column (Bio-Rad Laboratories, Inc., Hercules, CA, USA) operated at 65 °C with 0.01 N $H_2SO_4$ as mobile phase at 0.6 mL $min^{-1}$ in an Agilent 1100 HPLC system with refractive-index detection. The resulting glucose and cellobiose concentrations calculated (in mg $mL^{-1}$) for each digestion mixture was converted to *anhydro*-glucose and *anhydro*-cellobiose concentrations, respectively, by subtracting out the proportional weight added to each molecule by the water of hydrolysis. The sum of the concentrations of *anhydro*-glucose and *anhydro*-cellobiose, which sum is equivalent to the weight-concentration of the glucan chain that was hydrolyzed to produce the soluble sugars, was then divided by the initial weight-concentration of cellulose in the digestion mixture and multiplied by 100% to yield activity results as percent conversion of cellulose.

On pretreated biomass, it is possible that the non-cellulosic components could be oxidizing cysteine, and thus be responsible for the activity plateau seen in Fig. 1D. Thus, a control experiment was conducted wherein cysteine was added into the activity assay to result in a 10 mM addition every 24 h over 120 h Fig. S12† shows that the conversion of pretreated biomass with cysteine added periodically during the reaction does not change the activity relative to a procedure where cysteine is added only at the beginning of the reaction, as in Fig. 1D.

### TEM Sample preparation and imaging

Digested Avicel PH-101 samples were drop cast directly, without rinsing or additional treatment, on carbon-coated slot grids and negatively stained with 2% aqueous uranyl acetate. For immuno-EM, grids were placed on 10 μL drops of 2.5% non-fat dry milk in 1× PBS-0.1% Tween (PBST) for 30 min, then directly placed on ~10 μL drops, on parafilm, of primary antibodies diluted 1 : 50 in 1% milk PBST and incubated overnight at 4 °C. Following 3 × 1 min rinses, grids were placed on 10 μL drops of 2° antibody–15 nm gold conjugate (British BioCell) diluted 1 : 100 in PBST. Grids were then rinsed 3 × 1 min with PBST followed by water.

Pretreated and digested switchgrass samples were high-pressure frozen in 0.2 mm brass planchettes in a Leica EM PACT2 (Leica Microsystems GmbH, Wetzlar, Germany). Planchettes were placed in cryovials and freeze substitution took

 

place in a Leica AFS2 automatic freeze substitution unit in 2.5% glutaraldehyde w/v, 0.1% uranyl acetate w/v acetone for 4 days at −90 °C, increasing the temperature to −30 °C over 24 h, then increasing the temperature to 3 °C over 24 h. The fixation solution was replaced with 100% acetone and the temperature was then brought to 18 °C over 1 h. Samples were washed in 100% acetone for 1 h × 3, removed from their hats, and placed in BEEM capsules (BEEM Inc., Bronx, NY). LR White resin (EMS, Hatfield, PA) was added to the sample capsules in the follow concentrations v/v acetone: 25%, 50%, 75%, and 100% × 3 for 1 day each. Samples were then incubated in 100% LR White for 6 h and polymerized for 24 h at 60 °C in a nitrogen-purged vacuum oven. Sectioning was performed with a Diatome diamond knife (EMS, Hatfield, PA) on a Leica EM UTC ultramicrotome (Leica Microsystems GmbH, Wetzlar, Germany). All embedded samples were sectioned to a thickness of ~60 nm and collected on 0.35% Formvar-coated palladium/copper slot grids (SPI Supplies, West Chester, PA). Grids were post-stained for 4 min with 2% aqueous uranyl acetate and 2 min in 1% $KMnO_4$ to enhance lignin staining. Images were taken with a 4 mega-pixel Gatan UltraScan 1000 camera (Gatan, Pleasanton, CA) on a FEI Tecnai G2 20 Twin 200 kV LaB6 TEM (FEI, Hillsboro, OR).

Fiji (ImageJ) was used to perform image analysis on the TEM micrographs to calculate the 2D perimeter of the digested Avicel particles as an estimation of the actual 3D exposed surface area (Fig. S7†). Briefly, a region of interest measured 1 μm from the tapered or splayed end was thresholded to delineate the particle from the background carbon film. The thresholded image was converted to binary. Binary image process operators were used to ensure that a single Avicel particle was represented. These operators included one iteration for one count of the Close operation and one iteration of the Fill Holes tool. The Analyze Particles tool was then used to report the perimeter of the binary object within the defined region of interest.

## Acknowledgements

We acknowledge the U.S. Department of Energy Office of the Biomass Program (OBP) for funding the activity assays of complexed and noncomplexed cellulases, and the U.S. Department of Energy Office of Biological and Environmental Research through the BioEnergy Science Center (BESC), a DOE Bioenergy Research Center, for funding the TEM work. We thank a reviewer for detailed comments that improved the manuscript.

## Notes and references

1 L. R. Lynd, P. J. Weimer, W. H. van Zyl and I. S. Pretorius, *Microbiol. Mol. Biol. Rev.*, 2002, **66**, 739.
2 E. A. Bayer, J. P. Belaich, Y. Shoham and R. Lamed, *Annu. Rev. Microbiol.*, 2004, **58**, 521–554.
3 R. H. Doi and A. Kosugi, *Nat. Rev. Microbiol.*, 2004, **2**, 541–551.
4 A. L. Demain, M. Newcomb and J. H. D. Wu, *Microbiol. Mol. Biol. Rev.*, 2005, **69**, 124–154.
5 D. Martinez, R. M. Berka, B. Henrissat, M. Saloheimo, M. Arvas, S. E. Baker, J. Chapman, O. Chertkov, P. M. Coutinho, D. Cullen, E. G. J. Danchin, I. V. Grigoriev, P. Harris, M. Jackson, C. P. Kubicek, C. S. Han, I. Ho, L. F. Larrondo, A. L. de Leon, J. K. Magnuson, S. Merino, M. Misra, B. Nelson, N. Putnam, B. Robbertse, A. A. Salamov, M. Schmoll, A. Terry, N. Thayer, A. Westerholm-Parvinen, C. L. Schoch, J. Yao, R. Barbote, M. A. Nelson, C. Detter, D. Bruce, C. R. Kuske, G. Xie, P. Richardson, D. S. Rokhsar, S. M. Lucas, E. M. Rubin, N. Dunn-Coleman, M. Ward and T. S. Brettin, *Nat. Biotechnol.*, 2008, **26**, 553–560.
6 C. M. G. A. Fontes and H. J. Gilbert, *Annu. Rev. Biochem.*, 2010, **79**, 655–681.
7 G. Vaaje-Kolstad, B. Westereng, S. J. Horn, Z. Liu, H. Zhai, M. Sorlie and V. G. H. Eijsink, *Science*, 2010, **330**, 219–222.
8 S. P. S. Chundawat, G. T. Beckham, M. E. Himmel and B. E. Dale, *Annu. Rev. Chem. Biomol. Eng.*, 2011, **2**, 121–145.
9 R. J. Quinlan, M. D. Sweeney, L. Lo Leggio, H. Otten, J.-C. N. Poulsen, K. S. Johansen, K. B. R. M. Krogh, C. I. Jorgensen, M. Tovborg, A. Anthonsen, T. Tryfona, C. P. Walter, P. Dupree, F. Xu, G. J. Davies and P. H. Walton, *Proc. Natl. Acad. Sci. U. S. A.*, 2011, **108**, 15079–15084.
10 J. Lehtio, J. Sugiyama, M. Gustavsson, L. Fransson, M. Linder and T. T. Teeri, *Proc. Natl. Acad. Sci. U. S. A.*, 2003, **100**, 484–489.
11 C. Divne, J. Stahlberg, T. Reinikainen, L. Ruohonen, G. Pettersson, J. K. C. Knowles, T. T. Teeri and T. A. Jones, *Science*, 1994, **265**, 524–528.
12 B. G. Guimaraes, H. Souchon, B. L. Lytle, J. H. D. Wu and P. M. Alzari, *J. Mol. Biol.*, 2002, **320**, 587–596.
13 R. Lamed, E. Setter and E. A. Bayer, *J. Bacteriol.*, 1983, **156**, 828–836.
14 K. Kruus, A. C. Lua, A. L. Demain and J. H. D. Wu, *Proc. Natl. Acad. Sci. U. S. A.*, 1995, **92**, 9254–9258.
15 S. Pages, A. Belaich, C. Tardif, C. ReverbelLeroy, C. Gaudin and J. P. Belaich, *J. Bacteriol.*, 1996, **178**, 2279–2286.
16 M. Lemaire, H. Ohayon, P. Gounon, T. Fujino and P. Beguin, *J. Bacteriol.*, 1995, **177**, 2451–2459.
17 B. Raman, C. Pan, G. B. Hurst, M. Rodriguez, Jr, C. K. McKeown, P. K. Lankford, N. F. Samatova and J. R. Mielenz, *PLoS One*, 2009, **4**, e5271.
18 H. Chanzy and B. Henrissat, *FEBS Lett.*, 1985, **184**, 285–288.
19 H. Chanzy, B. Henrissat, R. Vuong and M. Schulein, *FEBS Lett.*, 1983, **153**, 113–118.
20 E. Morag, E. A. Bayer and R. Lamed, *Appl. Biochem. Biotechnol.*, 1992, **33**, 205–217.
21 E. A. Johnson and A. L. Demain, *Arch. Microbiol.*, 1984, **137**, 135–138.
22 A. L. Carvalho, F. M. V. Dias, J. A. M. Prates, T. Nagy, H. J. Gilbert, G. J. Davies, L. M. A. Ferreira, M. J. Romao and C. Fontes, *Proc. Natl. Acad. Sci. U. S. A.*, 2003, **100**, 13809–13814.
23 I. A. Kataeva, V. N. Uversky and L. G. Ljungdahl, *Biochem. J.*, 2003, **372**, 151–161.

24 E. A. Johnson, M. Sakajoh, G. Halliwell, A. Madia and A. L. Demain, *Appl. Environ. Microbiol.*, 1982, **43**, 1125–1132.
25 K. Kruus, A. Andreacchi, W. K. Wang and J. H. D. Wu, *Appl. Microbiol. Biotechnol.*, 1995, **44**, 399–404.
26 R. Lamed, R. Kenig, E. Morag, J. F. Calzada, F. Demicheo and E. A. Bayer, *Appl. Biochem. Biotechnol.*, 1991, **27**, 173–183.
27 A. Mittal, R. Katahira, M. E. Himmel and D. K. Johnson, *Biotechnol. Biofuels*, 2011, **4**.
28 B. S. Donohoe, S. R. Decker, M. P. Tucker, M. E. Himmel and T. B. Vinzant, *Biotechnol. Bioeng.*, 2008, **101**, 913–925.
29 *Cellic(R) CTec2 and HTec2 – Enzymes for hydrolysis of lignocellulosic materials*, Novozymes, 2010.
30 K. Igarashi, T. Uchihashi, A. Koivula, M. Wada, S. Kimura, T. Okamoto, M. Penttila, T. Ando and M. Samejima, *Science*, 2011, **333**, 1279–1282.
31 D. G. Olson, S. A. Tripathi, R. J. Giannone, J. Lo, N. C. Caiazza, D. A. Hogsett, R. L. Hettich, A. M. Guss, G. Dubrovsky and L. R. Lynd, *Proc. Natl. Acad. Sci. U. S. A.*, 2010, **107**, 17727–17732.
32 A. B. Boraston, D. N. Bolam, H. J. Gilbert and G. J. Davies, *Biochem. J.*, 2004, **382**, 769–781.
33 D. N. Bolam, H. F. Xie, P. White, P. J. Simpson, S. M. Hancock, M. P. Williamson and H. J. Gilbert, *Biochemistry*, 2001, **40**, 2468–2477.
34 A. B. Boraston, E. Kwan, P. Chiu, R. A. J. Warren and D. G. Kilburn, *J. Biol. Chem.*, 2003, **278**, 6120–6127.
35 A. B. Boraston, B. W. McLean, G. Chen, A. S. Li, R. A. J. Warren and D. G. Kilburn, *Mol. Microbiol.*, 2002, **43**, 187–194.
36 N. Cruys-Bagger, J. Elmerdahl, E. Praestgaard, H. Tatsumi, N. Spodsberg, K. Borch and P. Westh, *J. Biol. Chem.*, 2012, **287**, 18451–18458.
37 M. Kurasin and P. Valjamae, *J. Biol. Chem.*, 2011, **286**, 169–177.
38 W. T. Beeson, C. M. Phillips, J. H. D. Cate and M. A. Marletta, *J. Am. Chem. Soc.*, 2012, **134**, 890–892.
39 C. M. Phillips, W. T. Beeson, J. H. Cate and M. A. Marletta, *ACS Chem. Biol.*, 2011, **6**, 1399–1406.
40 B. Westereng, T. Ishida, G. Vaaje-Kolstad, M. Wu, V. G. H. Eijsink, K. Igarashi, M. Samejima, J. Stahlberg, S. J. Horn and M. Sandgren, *PLoS One*, 2011, **6**, e27807.
41 J. Rahikainen, S. Mikander, K. Marjamaa, T. Tamminen, A. Lappas, L. Viikari and K. Kruus, *Biotechnol. Bioeng.*, 2011, **108**, 2823–2834.
42 C. Boisset, C. Fraschini, M. Schulein, B. Henrissat and H. Chanzy, *Appl. Environ. Microbiol.*, 2000, **66**, 1444–1452.
43 R. Lamed, R. Kenig, E. Setter and E. A. Bayer, *Enzyme Microb. Technol.*, 1985, **7**, 37–41.
44 M. G. Resch, R. J. Giannone, R. L. Hettich, J. R. Mielenz, M. E. Himmel and Y. J. Bomble, 2012, in preparation.
45 P. V. Harris, D. Welner, K. C. McFarland, E. Re, J. C. N. Poulsen, K. Brown, R. Salbo, H. S. Ding, E. Vlasenko, S. Merino, F. Xu, J. Cherry, S. Larsen and L. Lo Leggio, *Biochemistry*, 2010, **49**, 3305–3316.
46 J. A. Langston, T. Shaghasi, E. Abbate, F. Xu, E. Vlasenko and M. D. Sweeney, *Appl. Environ. Microbiol.*, 2011, **77**, 7007–7015.
47 D. J. Schell, J. Farmer, M. Newman and J. D. McMillan, *Appl. Biochem. Biotechnol.*, 2003, **105–108**, 69–85.

 